Redox Biology 16 (2018) 344–351

Contents lists available at ScienceDirect

Redox Biology

journal homepage: www.elsevier.com/locate/redox

Short communication

Mitochondrial ROS cause motor deficits induced by synaptic inactivity: Implications for synapse pruning

Eva Sidlauskaite[a], Jack W. Gibson[a], Ian L. Megson[b], Philip D. Whitfield[b], Artak Tovmasyan[c], Ines Batinic-Haberle[c], Michael P. Murphy[d], Peter R. Moult[a], James N. Cobley[b,*]

[a] School of Science Engineering and Technology, Abertay University, Dundee DD1 1HG, UK
[b] Institute of Health Science, University of Highlands and Islands, Inverness IV2 3JH, UK
[c] Department of Radiation Oncology, School of Medicine, Duke University, Durham, NC 27710, USA
[d] MRC Mitochondrial Biology Unit, University of Cambridge, Cambridge Biomedical Campus, CB2 0XY, UK

ARTICLE INFO

Keywords:
Mitochondria
Reactive oxygen species
Synapse
Motor deficit
Neuromuscular junction
Xenopus

ABSTRACT

Developmental synapse pruning refines burgeoning connectomes. The basic mechanisms of mitochondrial reactive oxygen species (ROS) production suggest they select inactive synapses for pruning: whether they do so is unknown. To begin to unravel whether mitochondrial ROS regulate pruning, we made the local consequences of neuromuscular junction (NMJ) pruning detectable as motor deficits by using disparate exogenous and endogenous models to induce synaptic inactivity *en masse* in developing *Xenopus laevis* tadpoles. We resolved whether: (1) synaptic inactivity increases mitochondrial ROS; and (2) chemically heterogeneous antioxidants rescue synaptic inactivity induced motor deficits. Regardless of whether it was achieved with muscle (α-bungarotoxin), nerve (α-latrotoxin) targeted neurotoxins or an endogenous pruning cue (SPARC), synaptic inactivity increased mitochondrial ROS *in vivo*. The manganese porphyrins MnTE-2-PyP^{5+} and/or MnTnBuOE-2-PyP^{5+} blocked mitochondrial ROS to significantly reduce neurotoxin and endogenous pruning cue induced motor deficits. Selectively inducing mitochondrial ROS—using mitochondria-targeted Paraquat (MitoPQ)—recapitulated synaptic inactivity induced motor deficits; which were significantly reduced by blocking mitochondrial ROS with MnTnBuOE-2-PyP^{5+}. We unveil mitochondrial ROS as synaptic activity sentinels that regulate the phenotypical consequences of forced synaptic inactivity at the NMJ. Our novel results are relevant to pruning because synaptic inactivity is one of its defining features.

1. Introduction

Mitochondrial reactive oxygen species (ROS), namely superoxide anion ($O_2^{\cdot-}$) and hydrogen peroxide (H_2O_2), are of considerable biological interest because they can signal but can also cause damage [1–4]. The factors that control the production and removal of mitochondrial ROS are well understood (reviewed in [5–7]). ATP demand, [NADH] and proton motive force (Δp) control mitochondrial ROS production in forward mode whereas antioxidant enzyme activity controls their removal [5–10]. Key mitochondrial antioxidant enzymes include manganese superoxide dismutase, peroxiredoxin 3 and glutathione peroxidase 1 [11–13]. Using existing knowledge of mitochondrial ROS production and removal (the known), it is possible to make experimentally tractable predictions about situations wherein a role for mitochondrial ROS is suspected but unverified (the unknown).

Developmental synapse pruning refines burgeoning connectomes [14,15]. Neuronal activity regulates pruning: activity protects synapses from and inactivity selects synapses for pruning, respectively [16–18]. Mitochondrial ROS are proposed to regulate pruning because neuronal activity should divergently regulate their production [19,20]. Neuronal activity *should* fulfil essential criteria for comparatively low mitochondrial ROS production (i.e. high respiration, high ATP demand and low Δp [5]). Conversely, neuronal inactivity *should* fulfil essential criteria for significant mitochondrial ROS production in forward mode (i.e. low respiration, low ATP synthesis and [NADH] build-up [5]). In support, skeletal muscle activity and inactivity decreases and increases mitochondrial ROS, respectively [21–24]. Further, surgically abolishing skeletal muscle activity increases mitochondrial ROS *ex vivo* [25–28]. We propose that: mitochondrial ROS are endogenous synaptic activity sentinels.

Whether mitochondrial ROS regulate pruning is unknown because it is a novel idea associated with two formidable technical challenges. First, studying pruning is challenging in the brain owing it its intricate connectome. The neuromuscular junction (NMJ)—a peripheral synapse

* Corresponding author.
E-mail address: james.cobley@uhi.ac.uk (J.N. Cobley).

https://doi.org/10.1016/j.redox.2018.03.012
Received 20 February 2018; Received in revised form 15 March 2018; Accepted 17 March 2018
Available online 20 March 2018

between a motor neuron and skeletal muscle fibre—is an ideal alternative owing to its relative simplicity, size and accessibility [29]. The NMJ is tractable because its development requires pruning to transition from the poly to mono-innervated state [29–31]. Second, pruning occurs over a protracted time-course (order of weeks) and encompasses *in utero* and *ex utero* developmental stages [30]. It is, however, possible to use neurotoxins to broadly recapitulate pruning by forcing synaptic inactivity in species that develop *ex utero*, such as *Xenopus laevis* (*X. laevis*) [32]. Neurotoxins obviate the need for invasive surgical procedures that can provoke adaptive redox responses to injury [33–35]. A key advantage: neurotoxins make the micro functional outcomes of pruning (partial loss of innervation) detectable as motor deficits at the macro level owing to their mass action [36]. Whether they induce pruning is unclear; but their ability to, at worst, mimic its functional consequences (i.e. motor deficits owing to lost innervation) is clear. To begin to resolve whether mitochondrial ROS regulate pruning, we used multiple forced synaptic inactivity models to determine if: synaptic inactivity increases mitochondrial ROS; and chemically heterogeneous antioxidants rescue synaptic inactivity induced motor deficits.

2. Results

2.1. The manganese porphyrin MnTE-2-PyP^{5+} reduces α-BTX—a post-synaptic inactivity model—induced motor deficits

The neurotoxin α-bungarotoxin (α-BTX) induces forced synaptic inactivity by ligating the nicotinic acetylcholine receptor to competitively antagonise cholinergic neurotransmission ([36,37] Fig. 1A). We used α-BTX to induce forced synaptic inactivity in *X. leavis* tadpoles. To verify α-BTX induced motor deficits, we assessed evoked swimming frequency: α-BTX decreased evoked swimming frequency by 15.5 ± 1.4% compared to control (Fig. 1B). To determine if α-BTX increases mitochondrial ROS *in vivo*, we used two intensity based mitochondria-targeted (i.e. triphenylphosphonium cation conjugated) probes: mito-dihydroethidium (Mito-SOX) and mitochondria peroxy yellow 1 (MitoPY1) [38–40]. Free radicals (e.g. $O_2^{\cdot-}$) oxidise Mito-SOX to fluorescent ethidium or 2-hydroxyethidium products whereas H_2O_2 and/or peroxynitrite oxidise MitoPY1 to a fluorescent phenol by a boronate de-protection mechanism [41–47]. α-BTX increased Mito-SOX and MitoPY1 oxidation by 40.5 ± 4.9% and 30.5 ± 3.5%, respectively, compared to control (Fig. 1C-D).

To determine if mitochondrial ROS play a functional role, we used chemically heterogeneous antioxidants (Supplementary Table 1). Specifically, Mn(III) *meso*-tetrakis(2-pyridyl)porphyrin (MnTE-2-PyP^{5+}), Mn(III) *meso*-tetrakis(*N*-(*n*-butoxyethyl)pyridinium-2-yl (MnTnBuOE-2-PyP^{5+}), Mn(III) *meso*-tetrakis(4-carboxylatophenyl)porphyrin (MnTBAP^{3-}) and 2,2,6,6-tetramethyl-4-[5-(triphenylphosphonio)pentoxy] piperidin-1-oxy (MitoTempol) [48–52]. MnTBAP^{3-} and MitoTempol were inefficacious: failing to rescue α-BTX induced motor deficits or reduce MitoSOX and MitoPY1 oxidation. MnTnBuOE-2-PyP^{5+} successfully reduced MitoPY1 oxidation by 20.3 ± 4.2% compared to α-BTX, but failed to significantly reduce α-BTX induced MitoSOX oxidation or motor deficits. MnTE-2-PyP^{5+} successfully blocked mitochondrial ROS reducing Mito-SOX and MitoPY1 oxidation by 38.6 ± 4.7% and 31.2 ± 5.0%, respectively, compared to α-BTX (Fig. 1C-D). MnTE-2-PyP^{5+} significantly reduced α-BTX induced motor

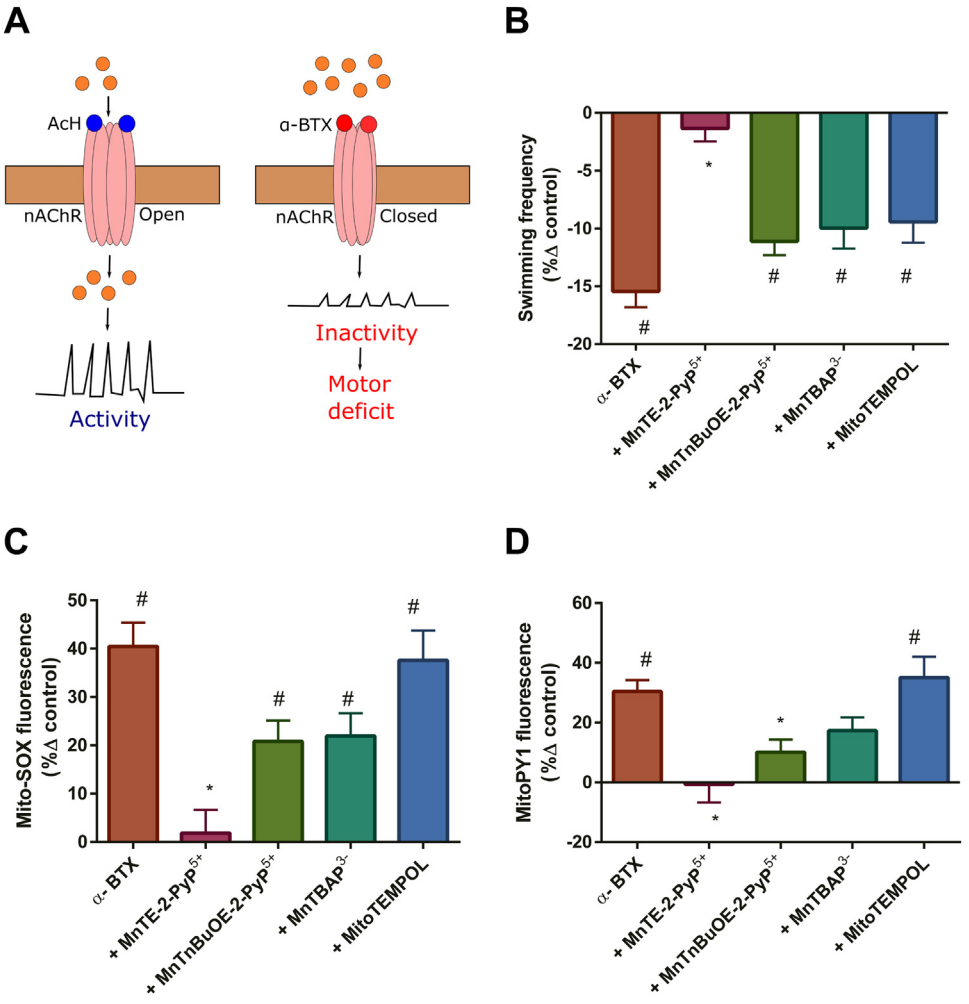

Fig. 1. α-BTX induced motor deficits are redox regulated. (A) α-BTX mechanism of action scheme. Left: skeletal muscle activity stems from acetylcholine (ACh) binding to post-synaptic nicotinic acetylcholine receptor (nAChR) to permit Na^+ entry. Right: α-BTX ligates the nAChR to render it impermeable to Na^+ leading to forced post-synaptic inactivity induced motor deficits. (B) Evoked swimming frequency (expressed as %δ control) by condition (α-BTX, α-BTX plus: MnTE-2-PyP^{5+}, MnTnBuOE-2-PyP^{5+}, MnTBAP^{3-} or MitoTempol; $n = 10$ in each condition). (C) Mito-SOX oxidation (expressed as %δ control) by condition ($n = 10$ per condition). (D) MitoPY1 oxidation (expressed as %δ control) by condition ($n = 10$ per condition). Error bars are SEM. Concentrations and incubations: α-BTX (8 μM for 30 min), MnTE-2-PyP^{5+}, MnTnBuOE-2-PyP^{5+}, MnTBAP^{3-} conditions = 1 μM for 30 min. MitoTempol = 20 μM for 30 min. # denotes significant difference vs control. * denotes significant difference vs α-BTX.

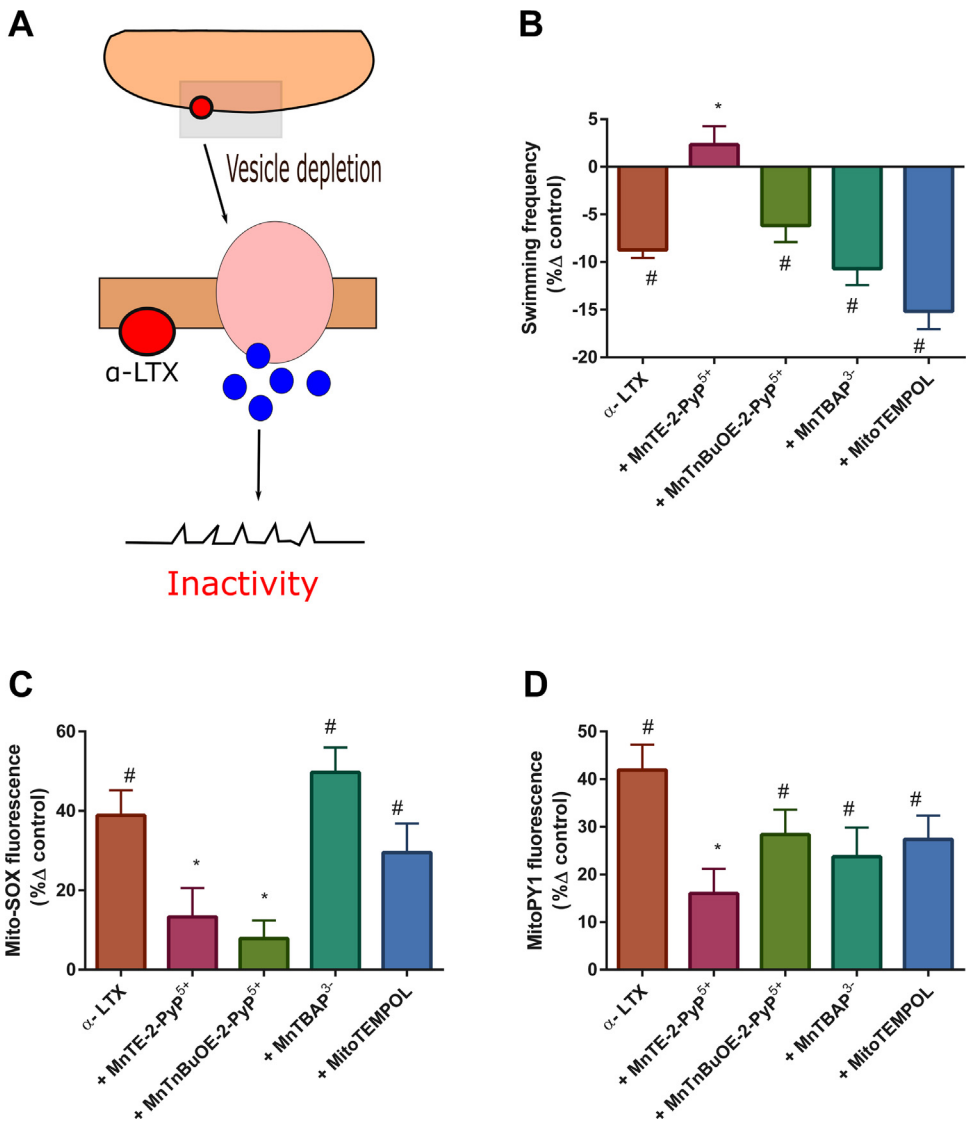

Fig. 2. α-LTX induced motor deficits are redox regulated. (A) α-LTX mechanism of action scheme. α-LTX binds to nerve terminals to cause mass neurotransmitter vesicle depletion, leading to pre-synaptic inactivity. (B) Evoked swimming frequency (expressed as %δ control) by condition (α-LTX, α-LTX plus: MnTE-2-PyP^{5+}, MnTnBuOE-2-PyP^{5+}, MnTBAP^{3-} or MitoTempol; $n = 10$ in each condition). (C) Mito-SOX oxidation (expressed as %δ control) by condition ($n = 10$ per condition). (D) MitoPY1 oxidation (expressed as %δ control) by condition ($n = 10$ per condition). Error bars are SEM. Concentrations and incubations: α-LTX (15 nM for 30 min), MnTE-2-PyP^{5+}, MnTnBuOE-2-PyP^{5+}, MnTBAP^{3-} conditions = 1 μM for 30 min. MitoTempol = 20 μM for 30 min. # denotes significant difference vs control. * denotes significant difference vs α-LTX.

deficits (Fig. 1B), restoring evoked swimming frequency to control values—no statistical difference between MnTE-2-PyP^{5+} and control.

2.2. The manganese porphyrin MnTE-2-PyP^{5+} abolishes α-LTX—a pre-synaptic inactivity model—induced motor deficits

The neurotoxin α-latrotoxin (α-LTX) forces pre-synaptic inactivity by binding to nerve terminals to cause mass Ca^{2+} influx, vesicle release and ATP depletion ([53–55] Fig. 2A). α-LTX induced motor deficits: reducing evoked swimming frequency by 8.3 ± 0.8% compared to control (Fig. 2B). To determine if α-LTX increased mitochondrial ROS, we assessed Mito-SOX and MitoPY1 oxidation. α-LTX increased Mito-SOX and MitoPY1 oxidation by 38.9 ± 6.3% and 41.9 ± 5.2%, respectively, compared to control (Fig. 2C-D). To determine if mitochondrial ROS were functional, we used antioxidants. MnTBAP^{3-} and MitoTempol were inefficacious: failing to rescue α-LTX induced motor deficits or reduce MitoSOX and MitoPY1 oxidation. MnTnBuOE-2-PyP^{5+} successfully reduced Mito-SOX oxidation but failed to significantly reduce α-LTX induced MitoPY1 oxidation or motor deficits. MnTE-2-PyP^{5+} decreased Mito-SOX and MitoPY1 oxidation by 25.6 ± 7.2% and 25.9 ± 5.1%, respectively, compared to α-LTX (Fig. 2C-D). MnTE-2-PyP^{5+} abolished α-LTX induced motor deficits (Fig. 2A-B).

2.3. MnTE-2-PyP^{5+} and MnTnBuOE-2-PyP^{5+} reduce SPARC—an endogenous pruning cue—induced motor deficits

Despite multiple advantages (e.g. known mechanisms) [36,37,53,54], neurotoxins lack physiological relevance beyond envenomation. Consequently, we used Secreted Protein Acidic and Rich in Cysteine (SPARC)—an endogenous pruning cue—to provide a physiologically relevant model ([56,57] Fig. 3A). SPARC reduced evoked swimming frequency by 12.0 ± 1.7% compared to control (Fig. 3B). To determine if SPARC increased mitochondrial ROS, we assessed Mito-SOX and MitoPY1 oxidation. SPARC increased Mito-SOX and MitoPY1 oxidation by 42.1 ± 5.5% and 49.5% ± 5.8%, respectively, compared to control (Fig. 3B-C). To determine if mitochondrial ROS were functional, we used antioxidants. MnTBAP^{3-} and MitoTempol were inefficacious: failing to rescue SPARC induced motor deficits or reduce MitoSOX and MitoPY1 oxidation. MnTE-2-PyP^{5+} and MnTnBuOE-2-PyP^{5+} blocked the SPARC induced increase in mitochondrial ROS. MnTE-2-PyP^{5+} and MnTnBuOE-2-PyP^{5+} reduced Mito-SOX (33.7 ± 4.2% and 28.77 ± 4.6%, respectively) and MitoPY1 (39.2 ± 4.8% and 38.17 ± 2.9%, respectively) oxidation compared to SPARC (Fig. 3C-D). MnTE-2-PyP^{5+} and MnTnBuOE-2-PyP^{5+} significantly reduced SPARC induced motor deficits (Fig. 3B), restoring evoked swimming frequency to control values—no statistical difference between MnTE-2-PyP^{5+} and MnTnBuOE-2-PyP^{5+} vs control.

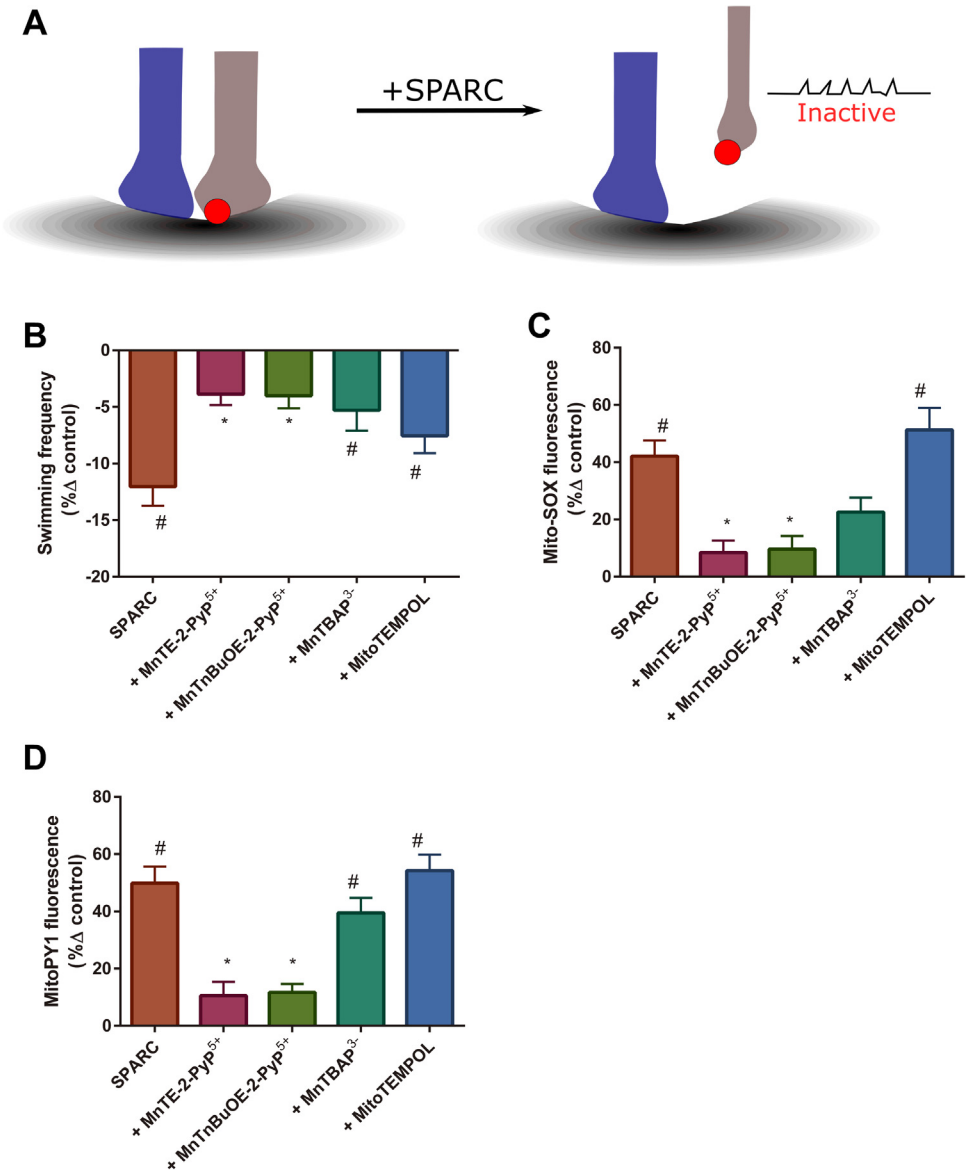

Fig. 3. SPARC induced motor deficits are redox regulated. (A) SPARC mechanism of action scheme. SPARC binds to weak synaptic inputs to selectively induce pruning—via a yet to be fully elucidated mechanism. Withdrawing inputs (retraction bulbs) are inactive; hence, global SPARC treatment can silence multiple NMJs to induce motor deficits. (B) Evoked swimming frequency (expressed as %δ control) by condition (SPARC, SPARC plus: MnTE-2-PyP^{5+}, MnTnBuOE-2-PyP^{5+}, MnTBAP^{3-} or MitoTempol; $n = 10$ in each condition). (C) Mito-SOX oxidation (expressed as %δ control) by condition ($n = 10$ per condition). (D) MitoPY1 oxidation (expressed as %δ control) by condition ($n = 10$ per condition). Error bars are SEM. Concentrations and incubations: SPARC (50 nM for 30 min), MnTE-2-PyP^{5+}, MnTnBuOE-2-PyP^{5+}, MnTBAP^{3-} conditions = 1 μM for 30 min. MitoTempol = 20 μM for 30 min. # denotes significant difference vs control. * denotes significant difference vs SPARC.

2.4. MitoPQ recapitulates exogenous and endogenous synaptic inactivity model induced motor deficits

If exogenous and endogenous forced synaptic inactivity models induce mitochondrial ROS, it should be possible to chemically recapitulate motor deficits by increasing their levels. A related advantage: one can leverage known redox chemistry to gain new insight regarding the redox control of forced synaptic inactivity. We used mitochondria-targeted paraquat (Mito-PQ) to selectively induce matrix $O_2^{\cdot-}$ [58] (Fig. 4A). Unlike respiratory chain inhibitors (e.g. rotenone [59]), MitoPQ leaves Δp and ATP synthesis unperturbed [58]. MitoPQ successfully increased mitochondrial ROS evidenced by increased Mito-SOX (44.7 ± 5.3%) and MitoPY1 (34.2 ± 4.3%) oxidation compared to control (Fig. 4B-C). MitoPQ decreased evoked swimming frequency by 19.9 ± 1.4% compared to control (Fig. 4D). We exclude the possibility that MitoPQ simply kills cells to induce motor deficits because primary muscle-nerve co-cultures remain viable after MitoPQ treatment (Supplementary Fig. 1). To explore the functional role of mitochondrial ROS, we used antioxidants. MnTnBuOE-2-PyP^{5+} reduced Mito-SOX (43.1 ± 4.2%) and MitoPY1 (51.3 ± 4.4%) oxidation compared to MitoPQ (Fig. 4B-C). MnTnBuOE-2-PyP^{5+} reduced MitoPQ induced motor deficits (Fig. 4D). Each antioxidant reduced MitoPQ induced motor deficits—perhaps due to MitoPQ indiscriminately targeting multiple cells consistent with greater (~ 5%) motor deficits compared with α-BTX, α-LTX and SPARC.

3. Discussion

If mitochondrial ROS are synaptic activity sentinels, their production should be unmasked by silencing synaptic activity. We robustly tested whether forced synaptic inactivity increases mitochondrial ROS using mechanistically diverse exogenous and endogenous models. Their ability to induce motor deficits—the canonical outcome of synaptic inactivity at the NMJ—was verified using a well-accepted behavioural assay, before we expolited the optical accessibility of *X. laevis* tadpoles to assess mitochondrial ROS *in vivo* using established techniques [38–45]. Forced synaptic inactivity rapidly (within 30 min) increases mitochondrial ROS *in vivo*, regardless of *how* it is achieved. The outcome is the *same* irrespective of whether one deploys muscle (α-BTX) or nerve (α-LTX) targeted neurotoxins or endogenous pruning cues (SPARC) to silence the NMJ. We acknowledge that global increases in mitochondrial ROS are described: specific roles of nerve or muscle mitochondria are important open questions. It will also be necessary to unravel how synaptic inactivity increases mitochondrial ROS with

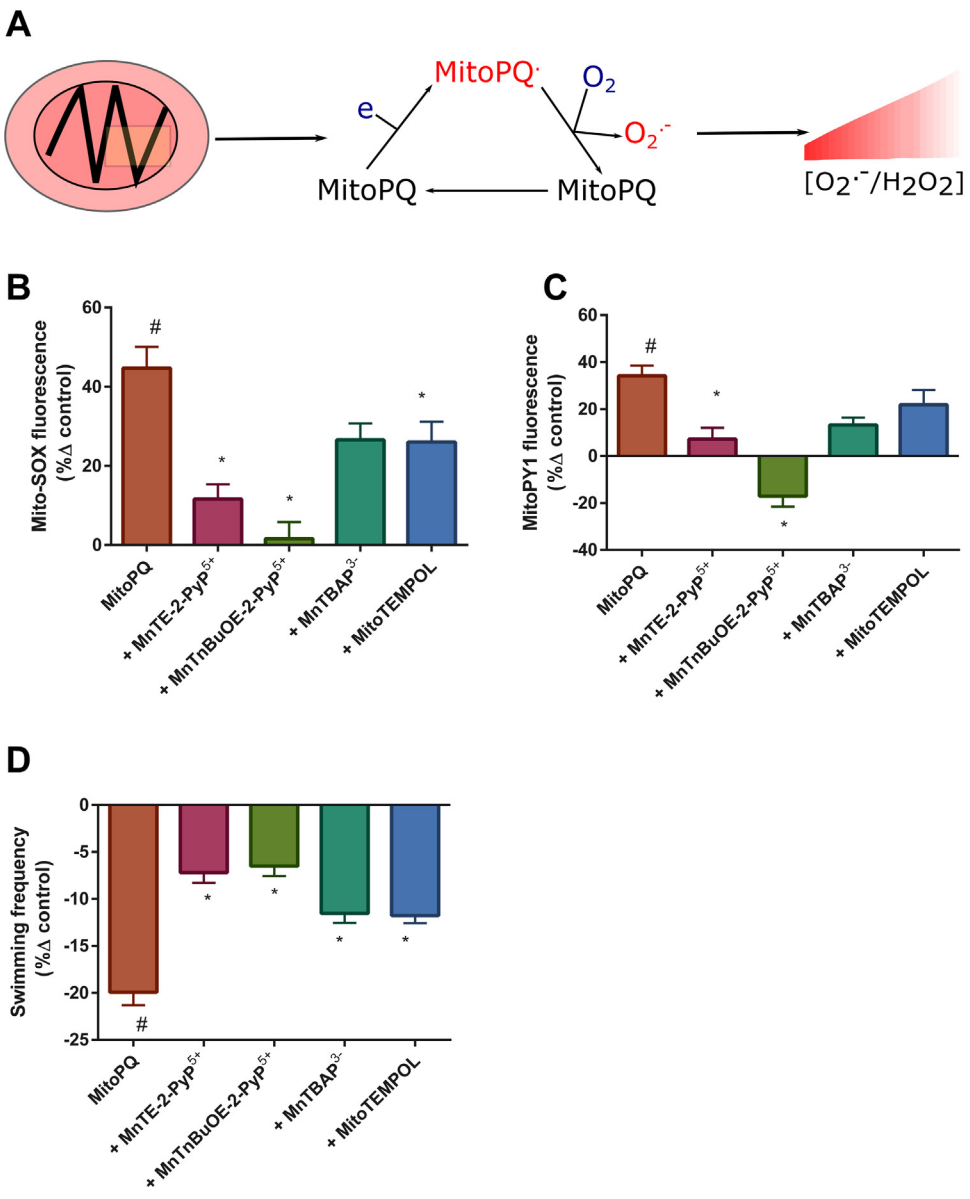

Fig. 4. MitoPQ induced motor deficits are redox regulated. (A) MitoPQ mechanism of action scheme. Within the mitochondrial matrix, MitoPQ accepts an electron from complex I to yield a MitoPQ radical. The MitoPQ radical reacts with molecular oxygen (O_2) to generate $O_2^{\cdot-}$, leading to an increase in matrix [$O_2^{\cdot-}$ and H_2O_2] (the latter as a consequence of MnSOD mediated $O_2^{\cdot-}$ dismutation). (B) Mito-SOX oxidation (expressed as %δ control) by condition (MitoPQ, MitoPQ plus: MnTE-2-PyP^{5+}, MnTnBuOE-2-PyP^{5+}, MnTBAP^{3-} or MitoTempol $n = 10$ per condition). (C) MitoPY1 oxidation (expressed as %δ control) by condition ($n = 10$ per condition). (D) Evoked swimming frequency (expressed as %δ control) by condition ($n = 10$ in each condition). Error bars are SEM. Concentrations and incubations: MitoPQ (5 μM for 60 min), MnTE-2-PyP^{5+}, MnTnBuOE-2-PyP^{5+}, MnTBAP^{3-} conditions = 1 μM for 30 min. MitoTempol = 20 μM for 30 min. #denotes significant difference vs control. *denotes significant difference vs MitoPQ.

reference to sites and modes of their production [5–7]. We are, however, the first to describe rapid increases in mitochondrial ROS *in vivo* across diverse synaptic inactivity models. That mechanistically diverse forced synaptic inactivity models increase mitochondrial ROS, supports the idea that mitochondrial ROS are endogenous synaptic activity sentinels.

Forcing synaptic inactivity *en masse* makes the phenotypical consequences of pruning (partial loss of innervation) at the micro level detectable as motor deficits at the macro level, enabling us to resolve whether mitochondrial ROS were functional or mere epiphenomena. Our forced synaptic inactivity models make functional studies possible because their effects are reversible [36,55]. If mitochondrial ROS are functional, antioxidants should rescue motor deficits, *provided* they block mitochondrial ROS [60–64]. The latter clause is key because failing to block mitochondrial ROS seemed to negate the ability of MnTBAP^{3-} and MitoTempol to reduce motor deficits induced by neurotoxins or SPARC. MnTE-2-PyP^{5+} and/or MnTnBuOE-2-PyP^{5+} block mitochondrial ROS to significantly reduce forced synaptic inactivity induced motor deficits. Consistent with their ability to accumulate in mitochondria and react with $O_2^{\cdot-}/H_2O_2$ [48,49,52,65]. However, given their pleiotropic redox biochemistry [48], how MnTE-2-PyP^{5+} and MnTnBuOE-2-PyP^{5+} act is an open question. MnTE-2-PyP^{5+} and/or MnTnBuOE-2-PyP^{5+} were effective *regardless* of how forced synaptic inactivity was achieved: significantly reducing motor deficits induced by disparate exogenous and endogenous models. Their efficacy suggests NMJ blockade fails to fully explain the motor deficits observed; perhaps, denervation contributes, consistent with synapse loss (pruning) as SPARCs *modus operandi* [56,57]. Our antioxidant studies strongly suggest that mitochondrial ROS cause forced synaptic inactivity induced motor deficits.

Multiple non-mitochondrial ROS sources exist (e.g. NADPH oxidase [66–68]); why, therefore, do we suspect a role for mitochondrial ROS? We include a role for non-mitochondrial ROS sources: ROS-induced ROS release means they likely contribute [69]. However, most do so at a *biological cost*: sustaining NADPH oxidase activity requires continued NADPH and GTP to supply electrons and activate RAC1, respectively [67,70,71]. We favour mitochondrial ROS as the proximal event because their production reports on ATP use without consuming it, placing mitochondrial ROS as energetically efficient synaptic activity sentinels [19,72–75]. We used MitoPQ to explore the role of mitochondrial ROS [58]. MitoPQ recapitulated synaptic inactivity induced motor deficits by increasing mitochondrial ROS. MnTnBuOE-2-PyP^{5+} blocked mitochondrial ROS to significantly reduce MitoPQ induced motor deficits; suggesting mitochondrial ROS production is the key

proximal event. A related corollary: MitoSNO rescues ischemia-reperfusion injury induced denervation by blocking mitochondrial ROS [76].

4. Conclusion

We unveil mitochondrial ROS as synaptic activity sentinels that regulate the phenotypical consequences (i.e. motor deficits) of forced synaptic inactivity at the NMJ. Our novel results are relevant to pruning because synaptic inactivity is one of its defining features.

5. Methods

5.1. Materials and reagents

Materials and reagents details are provided (Supplementary Table 2).

5.2. Xenopus laevis

X. laevis were reared in de-chlorinated water at room temperature. Nieuwkoop–Faber developmental stage 37–38 *X. laevis* tadpoles were used because the neural control of their swimming behaviour is well-understood [77]. Experiments received institutional ethical approval.

5.3. Treatments

In accordance with previous research [78,79], stage 37–38 *X. laevis* tadpoles were anesthetised in 0.1% MS-222 (3-aminobenzoic acid ester) in normal frog ringer (NFR, mM: 116 NaCl, 2 KCl, 1.8 $CaCl_2$, 5 Na^+-HEPES, pH 7.35) until their movement ceased (usually within a minute). MS-222 is commonly used to anesthetise *X. leavis* [80]. After mounting tadpoles on a Sylgaard stage immersed in NFR, a fine dorsal fin cut was made proximal to the myotomal region using a dissection knife to improve α-BTX and α-LTX permeability consistent with previous research [78,79,81,82]. After being allowed to recover for 30 min in NFR, tadpoles were incubated with either control (i.e. just NFR) or NFR plus: SPARC (50 nM for 30 min), α-LTX (15 nM for 30 min), α-BTX (8 μM for 30 min) or MitoPQ (5 μM for 60 min) in a light-protected Eppendorf before being washed in NFR for 3 min. For antioxidant experiments, tadpoles were pre-treated for 30 min with either MnTE-2-PyP^{5+} (1 μM), MnTnBuOE-2-PyP^{5+} (1 μM), $MnTBAP^{3-}$ (1 μM) and MitoTempol (20 μM) before being washed in NFR for 3 min and treated as described above. Doses and times were rationally selected based on pilot experiments and/or previous research [36,48–51,55,57,58].

5.4. Evoked swimming frequency

In accordance with previous research [78,83], evoked swimming was induced by manually touching the skin of *X. laevis* tadpoles with a pipette, which robustly initiates movement. Swimming was filmed at 400 frames per second with a Nikon D7100 camera and calculated as: swimming frequency = frames per second/ frames per cycle. A cycle defined one complete tail oscillation and the frames required to complete one cycle were manually counted to derive evoked swimming frequency. A single swimming episode was recorded at 2 min intervals [78], five episodes were recorded and their average calculated and defined as $n = 1$. Evoked swimming frequency experiments were performed during the day under room lighting because dimming lights influences swimming behaviour [83].

5.5. Mitochondrial ROS imaging

Mito-SOX and MitoPY1 were used at a working concentration of 5 μM [84]. After a 30 min light-protected incubation to avoid artificial photo-oxidation, tadpoles were washed in NFR supplemented with 0.1% MS-222 (to prevent movement while imaging) for 3 min and placed on a glass cavity slide with methylcellulose for whole-mount redox imaging in a dark room [84]. Care was taken to avoid bubbles when dispensing methylcellulose. If necessary, *X. laevis* tadpoles were orientated using nylon line [84], before being imaged (Mito-SOX excitation/emission: 510/580 nm; MitoPY1 excitation/emission: 488/517 nm) with a Lecia DMR epifluorescence microscope to capture images of the myotomal region (containing skeletal muscle and motor neurons) with a Nikon D7100 camera. For reference, Supplementary Fig. 4 shows the myotomal region. Regions of interest (ROIs) were analysed on Image J (http://imagej.nhi.gov/ij). Two images of the myotomal region were captured per tadpole and at least three ROIs were analysed per image. After background subtraction and smoothing [33], mean florescence intensity was calculated ($n = 1$ defines mean fluorescence per tadpole).

6. Primary muscle-nerve co-culture

To derive primary muscle-nerve co-cultures, Nieuwkoop–Faber Stage 22 *X. leavis* embryos were dissected in sterile NFR [85,86]. After removing the jelly coat and vitelline membrane with sterile forceps, the neural tube and associated myotomes were manually dissected in sterile Ca^{2+}/Mg^{2+}-free media (CMF mM: 125 NaCl, 2 KCl, 1.2 EDTA, 5 Na^+-HEPES, pH 7.35). Cells were left to dissociate in CMF for 2 h before being plated in poly-D-lysine coated (500 μg/ml) 35 mM glass culture dishes in media (50% L-15% and 50% NFR vol/vol) and cultured for 24 h at room temperature under ambient gas conditions before use.

6.1. Cell viability

Primary muscle-nerve co-cultures were treated with control (5 μM DMSO in media) or MitoPQ (5 μM in media) for 60 min before being incubated with Trypan blue solution (0.4% Trypan Blue stock diluted 1:1 with culture medium) for 2 min. After removing Trypan Blue solution, co-cultures were immediately fixed with 5% glutaraldehyde for 10 min at room temperature before being imaged using Leica DM IL LED. Images were captured using Leica MC120 HD Microscope Camera. Cell viability was calculated as: percentage viable cells = [1.00 – (Number of blue cells ÷ Number of total cells)] × 100.

6.2. Statistical analysis

To determine the appropriate statistical test, normal distribution was assessed using a Shapiro-Wilk test. Normally distributed data were analysed using a one-way general linear model with post-hoc Tukey tests. Abnormally distributed data were analysed using a non-parametric equivalent with Dunn's multiple comparison tests with alpha set to ≤ 0.05. Statistical analysis were performed on GraphPad PRISM 7 (https://www.graphpad.com/).

Acknowledgements

J.N.C. & P.R.M. acknowledge the generous financial support of the Carnegie Trust (R70103) and Royal Society (RG150598). J.N.C. thanks Dr Ania Noble (Portsmouth University) for kindly providing *X. laevis*. JNC is supported by Highlands and Islands Enterprise funding (HIEJNC007).

Conflict of interest

I.B.H is a consultant with and holds equities in BioMimetix JVLLC. I.B.H and Duke University have patent rights and have licensed technologies to BioMimetix JVLLC.

No other authors have any conflicts of interest to declare.

Author contributions

Conceptualization, J.N.C. and P.R.M; Methodology, E.S., J.N.C., P.R.M. and M.P.M; Investigation, E.S. and J.W.G; Writing – Original Draft, J.N.C; Writing – Review & Editing, ALL; Funding Acquisition, J.N.C. and P.R.M; Resources, M.P.M, A.T. and I.B.H; Supervision, J.N.C., M.P.M. I.L.M., P.D.W., I.B.H. and P.R.M.

Appendix A. Supplementary material

Supplementary data associated with this article can be found in the online version at http://dx.doi.org/10.1016/j.redox.2018.03.012.

References

[1] K.M. Holmström, T. Finkel, Cellular mechanisms and physiological consequences of redox-dependent signalling, Nat. Rev. Mol. Cell Biol. 15 (2014) 411–421, http://dx.doi.org/10.1038/nrm3801.

[2] Y. Collins, E.T. Chouchani, A.M. James, K.E. Menger, H.M. Cocheme, M.P. Murphy, Mitochondrial redox signalling at a glance, J. Cell Sci. 125 (2012), http://dx.doi.org/10.1242/jcs.110486 (1837–1837).

[3] L.A. Sena, N.S. Chandel, Physiological roles of mitochondrial reactive oxygen species, Mol. Cell. 48 (2012) 158–166, http://dx.doi.org/10.1016/j.molcel.2012.09.025.

[4] C.R. Reczek, N.S. Chandel, ROS-dependent signal transduction, Curr. Opin. Cell Biol. 33 (2015) 8–13, http://dx.doi.org/10.1016/j.ceb.2014.09.010.

[5] M.P. Murphy, How mitochondria produce reactive oxygen species, Biochem. J. 417 (2009) 1–13, http://dx.doi.org/10.1042/BJ20081386.

[6] J. Hirst, M.S. King, K.R. Pryde, The production of reactive oxygen species by complex I, Biochem. Soc. Trans. 36 (2008) 976–980, http://dx.doi.org/10.1042/BST0360976.

[7] M.D. Brand, Mitochondrial generation of superoxide and hydrogen peroxide as the source of mitochondrial redox signaling, Free Radic. Biol. Med. 100 (2016) 14–31, http://dx.doi.org/10.1016/j.freeradbiomed.2016.04.001.

[8] L. Kussmaul, J. Hirst, The mechanism of superoxide production by NADH: ubiquinone oxidoreductase (complex I) from bovine heart mitochondria, Proc. Natl. Acad. Sci. USA 103 (2006) 7607–7612.

[9] M.P. Murphy, Mitochondrial thiols in antioxidant protection and redox signaling: distinct roles for glutathionylation and other thiol modifications, Antioxid. Redox Signal. 16 (2012) 476–495, http://dx.doi.org/10.1089/ars.2011.4289.

[10] B. Halliwell, J.M.C. Gutteridge, Free Radicals in Biology & Medicine, Fifth ed., Oxford University Press, 2015.

[11] B. Keele, J. McCord, I. Fridovich, Superoxide dismutase from Escherichia coli B: a new manganese-containing enzyme, J. Biol. Chem. 245 (1970) 6175–6181.

[12] T.S. Chang, C.S. Cho, S. Park, S. Yu, W.K. Sang, G.R. Sue, Peroxiredoxin III, a mitochondrion-specific peroxidase, regulates apoptotic signaling by mitochondria, J. Biol. Chem. 279 (2004) 41975–41984, http://dx.doi.org/10.1074/jbc.M407707200.

[13] R. Brigelius-Flohé, M. Maiorino, Glutathione peroxidases, Biochim. Biophys. Acta - Gen. Subj. 1830 (2013) 3289–3303, http://dx.doi.org/10.1016/j.bbagen.2012.11.020.

[14] M. Costandi, Neuroplasticity, MIT Press, London, 2016.

[15] M.M. Riccomagno, A.L. Kolodkin, Sculpting neural circuits by axon and dendrite pruning, Annu. Rev. Cell Dev. Biol. 31 (2015) 779–805, http://dx.doi.org/10.1146/annurev-cellbio-100913-013038.

[16] M. Buffelli, R.W. Burgess, G. Feng, C.G. Lobe, J.W. Lichtman, J.R. Sanes, Genetic evidence that relative synaptic efficacy biases the outcome of synaptic competition, Nature 424 (2003) 430–434, http://dx.doi.org/10.1038/nature01836.1.

[17] H. Colman, J. Nabekura, J.W. Lichtman, Alterations in synaptic strength preceding axon withdrawal, Science 275 (80) (1997) (80-., 356–261).

[18] M.K. Walsh, J.W. Lichtman, S. Louis, In vivo time-lapse imaging of synaptic takeover associated with naturally occurring synapse elimination, Neuron 37 (2003) 67–73.

[19] J.N. Cobley, Synapse pruning: Mitochondrial ROS with their hands on shears, BioEssays. (n.d.).

[20] J.N. Cobley, M.-L. Fiorello, D.M. Bailey, 13 reasons why the brain is susceptible to oxidative stress, Redox Biol. 15 (2018) 490–503.

[21] R.L.S. Goncalves, C.L. Quinlan, I.V. Perevoshchikova, M. Hey-Mogensen, M.D. Brand, Sites of superoxide and hydrogen peroxide production by muscle mitochondria assessed ex vivo under conditions mimicking rest and exercise, J. Biol. Chem. 290 (2015) 209–227, http://dx.doi.org/10.1074/jbc.M114.619072.

[22] G.K. Sakellariou, A. Vasilaki, J. Palomero, A. Kayani, L. Zibrik, A. McArdle, M.J. Jackson, Studies of mitochondrial and nonmitochondrial sources implicate nicotinamide adenine dinucleotide phosphate oxidase(s) in the increased skeletal muscle superoxide generation that occurs during contractile activity, Antioxid. Redox Signal. 18 (2013) 603–621, http://dx.doi.org/10.1089/ars.2012.4623.

[23] J.N. Cobley, G.L. Close, D.M. Bailey, G.W. Davison, Exercise redox biochemistry: conceptual, methodological and technical recommendations, Redox Biol. 12 (2017) 540–548, http://dx.doi.org/10.1016/j.redox.2017.03.022.

[24] G.K. Sakellariou, M.J. Jackson, A. Vasilaki, Redefining the major contributors to superoxide production in contracting skeletal muscle. The role of NAD(P)H oxidases, Free Radic. Res. 48 (2014) 12–29, http://dx.doi.org/10.3109/10715762.2013.830718.

[25] F.L. Muller, W. Song, Y.C. Jang, Y. Liu, M. Sabia, A. Richardson, H. Van Remmen, Denervation-induced skeletal muscle atrophy is associated with increased mitochondrial ROS production, Am. J. Physiol. Regul. Integr. Comp. Physiol. 293 (2007) R1159–R1168, http://dx.doi.org/10.1152/ajpregu.00767.2006.

[26] A. Bhattacharya, F.L. Muller, Y. Liu, M. Sabia, H. Liang, W. Song, Y.C. Jang, Q. Ran, H. Van Remmen, Denervation induces cytosolic phospholipase a 2-mediated fatty acid hydroperoxide generation by muscle mitochondria, J. Biol. Chem. 284 (2009) 46–55, http://dx.doi.org/10.1074/jbc.M806311200.

[27] C. Karam, J. Yi, Y. Xiao, K. Dhakal, L. Zhang, X. Li, C. Manno, J. Xu, K. Li, H. Cheng, J. Ma, J. Zhou, Absence of physiological Ca2+ transients is an initial trigger for mitochondrial dysfunction in skeletal muscle following denervation, Skelet. Muscle 7 (2017) 6, http://dx.doi.org/10.1186/s13395-017-0123-0.

[28] N. Pollock, C.A. Staunton, A. Vasilaki, A. McArdle, M.J. Jackson, Denervated muscle fibers induce mitochondrial peroxide generation in neighboring innervated fibers: role in muscle aging, Free Radic. Biol. Med. 112 (2017) 84–92, http://dx.doi.org/10.1016/j.freeradbiomed.2017.07.017.

[29] J.R. Sanes, J.W. Lichtman, Induction, assembly, maturation and maintenance of a postsynaptic apparatus, Nat. Rev. Neurosci. 2 (2001) 791–805, http://dx.doi.org/10.1038/35097557/r35097557 (pii).

[30] J.C. Tapia, J.D. Wylie, N. Kasthuri, K.J. Hayworth, R. Schalek, D.R. Berger, C. Guatimosim, H.S. Seung, J.W. Lichtman, Pervasive synaptic branch removal in the mammalian neuromuscular system at birth, Neuron 74 (2012) 816–829, http://dx.doi.org/10.1016/j.neuron.2012.04.017.

[31] M.S. Brill, T. Kleele, L. Ruschkies, M. Wang, N.A. Marahori, M.S. Reuter, T.J. Hausrat, E. Weigand, M. Fisher, A. Ahles, S. Engelhardt, D.L. Bishop, M. Kneussel, T. Misgeld, Branch-specific microtubule destabilization mediates axon branch loss during neuromuscular synapse elimination, Neuron 92 (2016) 845–856, http://dx.doi.org/10.1016/j.neuron.2016.09.049.

[32] R.M. Harland, R.M. Grainger, Xenopus research: metamorphosed by genetics and genomics, Trends Genet. 27 (2011) 507–515, http://dx.doi.org/10.1016/j.tig.2011.08.003.

[33] N.R. Love, Y. Chen, S. Ishibashi, P. Kritsiligkou, R. Lea, Y. Koh, J.L. Gallop, K. Dorey, E. Amaya, Amputation-induced reactive oxygen species are required for successful Xenopus tadpole tail regeneration, Nat. Cell Biol. 15 (2013) 222–228, http://dx.doi.org/10.1038/ncb2659.

[34] R. Zhou, A.S. Yazdi, P. Menu, J. Tschopp, A role for mitochondria in NLRP3 inflammasome activation, Nature 469 (2011) 221–226, http://dx.doi.org/10.1038/nature09663.

[35] P. Niethammer, C. Grabher, a.T. Look, T.J. Mitchison, A tissue-scale gradient of hydrogen peroxide mediates rapid wound detection in zebrafish, Nature 459 (2009) 996–999, http://dx.doi.org/10.1038/nature08119.

[36] M. Akaaboune, S.M. Culican, S.G. Turney, J.W. Lichtman, Rapid and reversible effects of activity on acetylcholine receptor density at the neuromuscular junction in vivo, Science 286 (1999) 503–507 (doi:7909)(pii) (80-.).

[37] R.J. Balice-Gordon, J.W. Lichtman, Long-term synapse loss induced by focal blockade of postsynaptic receptors, Nature 372 (1994) 519–524.

[38] K.M. Robinson, M.S. Janes, M. Pehar, J.S. Monette, M.F. Ross, T.M. Hagen, M.P. Murphy, J.S. Beckman, Selective fluorescent imaging of superoxide in vivo using ethidium-based probes, Proc. Natl. Acad. Sci. USA 103 (2006) 15038–15043, http://dx.doi.org/10.1073/pnas.0601945103.

[39] B.C. Dickinson, C.J. Chang, A targetable fluorescent probe for imaging hydrogen peroxide in the mitochondria of living cells, J. Am. Chem. Soc. 130 (2008) 9638–9639, http://dx.doi.org/10.1021/ja802355u.

[40] R. Smith, R.C. Hartley, M.P. Murphy, Mitochondria-targeted small molecule therapeutics and probes, Antioxid. Redox Signal. 15 (2011) 3021–3038.

[41] M.M. Shchepinova, A.G. Cairns, T.A. Prime, A. Logan, A.M. James, A.R. Hall, S. Vidoni, S. Arndt, S.T. Caldwell, H.A. Prag, V.R. Pell, T. Krieg, J.F. Mulvey, P. Yadav, J.N. Cobley, T.P. Bright, H.M. Senn, R.F. Anderson, M.P. Murphy, R.C. Hartley, MitoNeoD, A mitochondria-targeted superoxide probe, Cell Chem. Biol. 3 (2017) 8–21, http://dx.doi.org/10.1016/j.chembiol.2017.08.003.

[42] B. Kalyanaraman, V. Darley-Usmar, K.J.A. Davies, P.A. Dennery, H.J. Forman, M.B. Grisham, G.E. Mann, K. Moore, L.J. Roberts, H. Ischiropoulos, Measuring reactive oxygen and nitrogen species with fluorescent probes: challenges and limitations, Free Radic. Biol. Med. 52 (2012) 1–6, http://dx.doi.org/10.1016/j.freeradbiomed.2011.09.030.

[43] J. Zielonka, B. Kalyanaraman, Hydroethidine- and MitoSOX-derived red fluorescence is not a reliable indicator of intracellular superoxide formation: another inconvenient truth, Free Radic. Biol. Med. 48 (2010) 983–1001, http://dx.doi.org/10.1016/j.freeradbiomed.2010.01.028.

[44] E.W. Miller, A.E. Albers, C.J. Chang, Boronate based fluorescent probes for imaging cellular hydrogen peroxide, J. Am. Chem. Soc. 127 (2005) 16652–16659, http://dx.doi.org/10.1021/ja054474f.

[45] A. Sikora, J. Zielonka, M. Lopez, J. Joseph, B. Kalyanaraman, Direct oxidation of boronates by peroxynitrite: mechanism and implications in fluorescence imaging of peroxynitrite, Free Radic. Biol. Med. 47 (2009) 1401–1407, http://dx.doi.org/10.1016/j.freeradbiomed.2009.08.006.

[46] C. Prolo, N. Rios, L. Piacenza, M.N. Álvarez, R. Radi, Fluorescence and chemiluminescence approaches for peroxynitrite detection, Free Radic. Biol. Med. (2018), http://dx.doi.org/10.1016/j.freeradbiomed.2018.02.017.

[47] C.C. Winterbourn, Biological production, detection, and fate of hydrogen peroxide, Antioxid. Redox Signal (2017).

[48] I. Batinic-Haberle, A. Tovmasyan, E.R.H. Roberts, Z. Vujaskovic, K.W. Leong, I. Spasojevic, S.O.D. Therapeutics, Latest insights into their structure-activity relationships and impact on the cellular redox-based signaling pathways, Antioxid.

Redox Signal. 20 (2014) 2372–2415, http://dx.doi.org/10.1089/ars.2012.5147.
[49] I. Batinic-Haberle, A. Tovmasyan, I. Spasojevic, An educational overview of the chemistry, biochemistry and therapeutic aspects of Mn porphyrins – from superoxide dismutation to H2O2-driven pathways, Redox Biol. 5 (2015) 43–65, http://dx.doi.org/10.1016/j.redox.2015.01.017.
[50] J. Trnka, F.H. Blaikie, R.A.J. Smith, M.P. Murphy, A mitochondria-targeted nitroxide is reduced to its hydroxylamine by ubiquinol in mitochondria, Free Radic. Biol. Med. 44 (2008) 1406–1419, http://dx.doi.org/10.1016/j.freeradbiomed.2007.12.036.
[51] J. Trnka, F.H. Blaikie, A. Logan, R.A.J. Smith, M.P. Murphy, Antioxidant properties of MitoTEMPOL and its hydroxylamine, Free Radic. Res. 43 (2009) 4–12, http://dx.doi.org/10.1080/10715760802582183.
[52] I. Batinić-Haberle, J.S. Rebouças, I. Spasojević, Superoxide dismutase mimics: chemistry, pharmacology, and therapeutic potential, Antioxid. Redox Signal. 13 (2010) 877–918, http://dx.doi.org/10.1089/ars.2009.2876.
[53] M. Rigoni, Equivalent effects of snake PLA2 neurotoxins and lysophospholipid-fatty acid mixtures, Science 310 (2005) 1678–1680, http://dx.doi.org/10.1126/science.1120640 (80-.).
[54] M. Rigoni, M. Paoli, E. Milanesi, P. Caccin, A. Rasola, P. Bernardi, C. Montecucco, Snake phospholipase A2 neurotoxins enter neurons, bind specifically to mitochondria, and open their transition pores, J. Biol. Chem. 283 (2008) 34013–34020, http://dx.doi.org/10.1074/jbc.M803243200.
[55] E. Duregotti, S. Negro, M. Scorzeto, I. Zornetta, B.C. Dickinson, C.J. Chang, C. Montecucco, M. Rigoni, Mitochondrial alarmins released by degenerating motor axon terminals activate perisynaptic Schwann cells, Proc. Natl. Acad. Sci. USA 112 (2015) E497–E505, http://dx.doi.org/10.1073/pnas.1417108112.
[56] H. Kucukdereli, N.J. Allen, A.T. Lee, A. Feng, M.I. Ozlu, L.M. Conatser, C. Chakraborty, G. Workman, M. Weaver, E.H. Sage, B.A. Barres, C. Eroglu, Control of excitatory CNS synaptogenesis by astrocyte-secreted proteins Hevin and SPARC, Proc. Natl. Acad. Sci. USA 108 (2011) E440–E449, http://dx.doi.org/10.1073/pnas.1104977108.
[57] F.J. López-Murcia, B. Terni, A. Llobet, SPARC triggers a cell-autonomous program of synapse elimination, Proc. Natl. Acad. Sci. USA 112 (2015) 13366–13371, http://dx.doi.org/10.1073/pnas.1512202112.
[58] E.L. Robb, J.M. Gawel, D. Aksentijevic, H.M. Cocheme, T.S. Stewart, M.M. Shchepinova, H. Qiang, T.A. Prime, T.P. Bright, A.M. James, M.J. Shattock, H.M. Senn, R.C. Hartley, M.P. Murphy, Selective superoxide generation within mitochondria by the targeted redox cycler MitoParaquat, Free Radic. Biol. Med. 89 (2015) 883–894, http://dx.doi.org/10.1016/j.freeradbiomed.2015.08.021.
[59] A.L. Orr, L. Vargas, C.N. Turk, J.E. Baaten, J.T. Matzen, V.J. Dardov, S.J. Attle, J. Li, D.C. Quackenbush, R.L.S. Goncalves, I.V. Perevoshchikova, H.M. Petrassi, S.L. Meeusen, E.K. Ainscow, M.D. Brand, Suppressors of superoxide production from mitochondrial complex III, Nat. Chem. Biol. 11 (2015) 834–839, http://dx.doi.org/10.1038/nchembio.1910.
[60] M.P. Murphy, Antioxidants as therapies: can we improve on nature? Free Radic. Biol. Med. 66 (2014) 20–23, http://dx.doi.org/10.1016/j.freeradbiomed.2013.04.010.
[61] B.J. Day, Antioxidant therapeutics: pandoras box, Free Radic. Biol. Med. 66 (2014) 58–64, http://dx.doi.org/10.1016/j.freeradbiomed.2013.05.047.
[62] H.J. Forman, K.J. a. Davies, F. Ursini, How do nutritional antioxidants really work: nucleophilic tone and para-hormesis versus free radical scavenging in vivo, Free Radic. Biol. Med. 66 (2014) 24–35, http://dx.doi.org/10.1016/j.freeradbiomed.2013.05.045.
[63] J.N. Cobley, H. McHardy, J.P. Morton, M.G. Nikolaidis, G.L. Close, Influence of vitamin C and vitamin E on redox signalling: implications for exercise adaptations, Free Radic. Biol. Med. 84 (2015) 65–76, http://dx.doi.org/10.1016/j.freeradbiomed.2015.03.018.
[64] J.M.C. Gutteridge, B. Halliwell, Antioxidants: molecules, medicines, and myths, Biochem. Biophys. Res. Commun. 393 (2010) 561–564, http://dx.doi.org/10.1016/j.bbrc.2010.02.071.
[65] Z. Rajic, A. Tovmasyan, I. Spasojevic, H. Sheng, M. Lu, A.M. Li, E.B. Gralla, D.S. Warner, L. Benov, I. Batinic-Haberle, A new SOD mimic, Mn(III) ortho N-butoxyethylpyridylporphyrin, combines superb potency and lipophilicity with low toxicity, Free Radic. Biol. Med. 52 (2012) 1828–1834, http://dx.doi.org/10.1016/j.freeradbiomed.2012.02.006.
[66] C.C. Winterbourn, Reconciling the chemistry and biology of reactive oxygen species, Nat. Chem. Biol. 4 (2008) 278–286, http://dx.doi.org/10.1038/nchembio.85.
[67] K. Bedard, K. Krause, The NOX family of ROS-generating NADPH oxidases: physiology and pathophysiology, Physiol. Rev. 87 (2007) 245–313, http://dx.doi.org/10.1152/physrev.00044.2005.
[68] D.P. Jones, H. Sies, The redox code, Antioxid. Redox Signal. 23 (2015) 734–746, http://dx.doi.org/10.1089/ars.2015.6247.
[69] D.B. Zorov, M. Juhaszova, S.J. Sollott, Mitochondrial reactive oxygen species (ROS) and ROS-induced ROS release, Physiol. Rev. 94 (2014) 909–950, http://dx.doi.org/10.1152/physrev.00026.2013.
[70] B.M. Babior, J.D. Lambeth, W. Nauseef, The neutrophil NADPH oxidase, Arch. Biochem Biophys. 397 (2002) 342–344, http://dx.doi.org/10.1006/abbi.2001.2642.
[71] J.D. Lambeth, NOX enzymes and the biology of reactive oxygen, Nat. Rev. Immunol. 4 (2004) 181–189, http://dx.doi.org/10.1038/nri1312.
[72] G. Barja, Oxygen radicals, a failure or success of evolution, Free Radic. Res. 18 (1993) 63–70.
[73] G. Barja, Updating the mitochondrial free radical theory of aging: an integrated view, key aspects and confounding concepts, Antioxid. Redox Signal. 19 (2013) 1420–1445, http://dx.doi.org/10.1089/ars.2012.5148.
[74] N. Lane, Oxygen: The Molecule That Made the World, Oxford University Press, Oxford, 2002.
[75] N. Lane, Mitonuclear match: optimizing fitness and fertility over generations drives ageing within generations, BioEssays 33 (2011) 860–869, http://dx.doi.org/10.1002/bies.201100051.
[76] R.J. Wilson, J.C. Drake, D. Cui, B.M. Lewellen, C.C. Fisher, M. Zhang, D.F. Kashatus, L.A. Palmer, M.P. Murphy, Z. Yan, Mitochondrial protein S- nitrosation protects against ischemia reperfusion-induced denervation at neuromuscular junction in skeletal muscle, Free Radic. Biol. Med. 117 (2018) 180–190, http://dx.doi.org/10.1016/j.freeradbiomed.2018.02.006.
[77] P.D. Nieuwkoop, J. Faber, Normal Table of Xenopus Laevis (Daudin): A Systematical and Chronological Survey of a Development from a Fertilized Egg until the End of Metamorphosis, Garland Publising, 1994.
[78] H.-Y. Zhang, W.-C. Li, W.J. Heitler, K.T. Sillar, Electrical coupling synchronises spinal motoneuron activity during swimming in hatchling Xenopus tadpoles, J. Physiol. 587 (2009) 4455–4466, http://dx.doi.org/10.1113/jphysiol.2009.173468.
[79] H. Zhang, J. Issberner, K.T. Sillar, Development of a spinal locomotor rheostat, Proc. Natl. Acad. Sci. USA 108 (2011) 11674–11679, http://dx.doi.org/10.1073/pnas.1018512108.
[80] H.L. Sive, R.M. Grainger, R.M. Harland, Early Development of Xenopus laevis: A Laboratory Manual, First edition, Cold Spring Harbor Laboratory Press, New York, 2000.
[81] W. Li, P.R. Moult, The control of locomotor frequency by excitation and inhibition, J. Neurosci. 32 (2012) 6220–6230, http://dx.doi.org/10.1523/JNEUROSCI.6289-11.2012.
[82] P.R. Moult, G.A. Cottrell, W. Li, Fast silencing reveals a lost role for reciprocal inhibition in locomotion, Neuron 77 (2013) 129–140, http://dx.doi.org/10.1016/j.neuron.2012.10.040.
[83] A. Roberts, W.-C. Li, S.R. Soffe, How neurons generate behaviour in a hatchling amphibian tadpole: an outline, Front. Behav. Neurosci. 4 (2010) 16, http://dx.doi.org/10.3389/fnbeh.2010.00016.
[84] V. Mugoni, A. Camporeale, M.M. Santoro, Analysis of oxidative stress in zebrafish embryos, J. Vis. Exp. 89 (2014) 1–11, http://dx.doi.org/10.3791/51328.
[85] B. Yazejian, R.M. Yazejian, R. Einarsson, A.D. Grinnell, Simultaneous pre- and post-synaptic electrophysiological recording from Xenopus nerve-muscle co-cultures, J. Vis. Exp. 73 (2013) 1–6, http://dx.doi.org/10.3791/50253.
[86] T.M. Gómez, D. Harrigan, J. Henley, E. Robles, Working with Xenopus spinal neurons in live cell culture, Methods Cell Biol. 71 (2003) 129–156, http://dx.doi.org/10.1016/S0091-679X(03)01008-2.